

Steven Labalme

TA: Ben Masters

Lab partners: Joe Geniesse, Irene Madejski, and Sophia Madejski

16-23 February 2023

2 March 2023

6 ANALYSIS OF THE ELECTROCATALYTIC ACTIVITY OF PLATINUM, TIN, AND TITANIUM TOWARD THE HYDROGEN EVOLUTION REACTION

Abstract

The goal of this experiment is to evaluate three candidates for the electrocatalysis of the hydrogen evolution reaction (a reaction in which there is broad chemical and societal interest), and to probe the mechanism over each of metal to determine which of two well-defined types is active. It was determined that the order of catalytic activity is platinum, then titanium, then tin. Additionally, it was determined that platinum follows the Volmer-Tafel mechanism with second-order reaction kinetics in the concentration of acid, and tin follows the Volmer-Heyrovsky mechanism with first-order kinetics in said concentration. Altogether, the data suggests that the metal-hydride bond strength is a key indicator of the rate of the hydrogen evolution reaction, providing a key tool necessary to design future reactions.

Introduction

The constantly increasing societal demand for energy coupled with the perils of climate change demand investment in sustainable, fossil-fuel free sources of energy. One direction that has been attracting increasing interest is electrochemistry; promising experiments suggest that important problems in chemical synthesis, renewable energy, energy storage, and more may be able to be solved using such an approach.¹ For example, means of harnessing the carbon dioxide reduction reaction to store wind and solar energy have been devised and implemented at small scales.²

Electrochemistry is particularly interesting because it is comparably simple to probe the mechanisms of electrochemical reactions, a rarity in chemistry.² For example, the reaction rate is always directly measurable via its direct proportionality with the flowing current. Indeed, since the mechanisms are well-understood, rational design of experiments is commonplace. For example, a molecular-level understanding of the hydrogen evolution reaction (HER) allows scientists to predict that changing the concentration of an acid *molecule* (the hydronium producing species) will affect the reaction rate, but changing the level of hydrogen itself will not. The HER is as follows.



In fact, the HER is particularly notable for several more reasons. Most importantly, it

is key to the production of hydrogen, a promising alternative fuel and valuable commodity chemical. Additionally, it has a very simple mechanism, so strategies to control and manipulate it can be evaluated in theory with relative ease. Thus, optimizing the HER is both desirable (because of its importance in chemistry) and theoretically feasible (because of its simple mechanism). Two important strategies to this effect are (1) selecting the best possible catalyst material and (2) determining which of the two possible mechanisms (Volmer-Tafel [V-T] and Volmer-Heyrovsky [V-H])³ is active for a given catalyst material. Both strategies will be worked through herein. The first will be discussed in greater detail presently.

In this study, the researchers will evaluate the electrocatalytic properties of three transition metals: platinum (Pt), tin (Sn), and titanium (Ti). Transition metals are natural candidates for electrocatalysts because of their incompletely filled *d* orbitals, which enable them to donate and accept electrons with a minimal energy penalty. Using cyclic voltammetry (CV), the overpotential η needed to initiate the catalytic reaction will be determined. Measuring against an Hg/HgSO₄ electrode with a potential of 0.650 V vs SHE (SHE is the standard hydrogen electrode, which is the potential of the HER in 1 M acid conditions and under 1 atm of H₂), all data will need to be converted to SHE via

$$E_{\text{SHE}} = E_{\text{Hg/HgSO}_4} + 0.650 \quad (2)$$

All quantities above are in V, a measure of electric potential. The overpotential, specifically, is then given by

$$\eta = E_{\text{H}^+/\text{H}_2} - E_{\text{app}} \quad (3)$$

where $E_{\text{H}^+/\text{H}_2} = 0$ is the potential of the HER vs SHE and E_{app} is the potential applied to induce catalysis. All quantities are, again, in V.

The magnitude of the overpotential reflects the magnitude of the kinetic barriers preventing a particular metal from engaging in catalysis. Thus, it is inversely proportional to the activity of the catalysts, with higher overpotentials signifying greater element-specific kinetic barriers and thus lower activity.

Additionally, the overpotential aids in the design of the subsequent chronoamperometry (CA) experiments. CA data can be collected in the vicinity of the onset potential to enable the construction of a *Tafel plot*. The slope of the line of best fit in this plot is related to some key quantitative differentiators between the V-T and V-H mechanisms, so making one allows for the determination of the active mechanism.

In particular, a Tafel plot plots applied potential on the *y*-axis and the base 10 logarithm of the negative of *current density* on the *x*-axis. Note that the current density is denoted by

j and defined as follows, where I is current and A is geometric surface area.

$$j = \frac{I}{A} \quad (4)$$

Current density is an *intensive* property of the given substance (metal) and is thus a better, normalized measure of activity than raw intensity I , an *extensive* property. It is measured in mA/cm². By definition, it encapsulates the amount of electrons flowing through a unit of area in a given amount of time.

Returning to Tafel plots, the Tafel slope can be related to the molecular parameters as follows.⁴ Begin with the equation

$$j = j_0 e^{\beta \eta F / RT} \quad (5)$$

where j is the measured current density, j_0 is the initial current density, β is the symmetry factor (a unitless measure of the reorganization energy in solution), η is the overpotential, $F = eN_A$ is Faraday's constant, R is the ideal gas constant, and T is temperature. Rearranging, the following is obtained.

$$\begin{aligned} j_0 e^{\beta \eta F / RT} &= j \\ \frac{\beta \eta F}{RT} \log_{10}(e) &= \log_{10} \frac{j}{j_0} \\ \eta &= \frac{1}{\log_{10}(e)} \frac{RT}{\beta F} [\log_{10}(j) - \log_{10}(j_0)] \\ &= 2.3 \frac{RT}{\beta F} [\log_{10}(j) - \log_{10}(j_0)] \end{aligned} \quad (6)$$

Thus, the expected slope of the Tafel plot in terms of molecular parameters is $2.3RT/\beta F$. It follows via consideration of both mechanisms that

$$\frac{2.3RT}{\beta F} = 30 \text{ mV}/\log(j) \quad (7)$$

if the V-T mechanism is active

$$\frac{2.3RT}{\beta F} = 120 \text{ mV}/\log(j) \quad (8)$$

if the V-H mechanism is active. All data fittings will be performed in Excel with a linear regression.

Essentially, the researchers seek herein to determine both which catalyst (between Pt, Sn, and Ti) is the most active and which mechanism (V-T or V-H) is active for Pt and Sn using cyclic voltammetry and the evaluation of the slope of a relevant Tafel plot.

Experimental

The experimental setup used herein centered around a Gamry potentiostat. This device enables the application of precise voltages and the measurement of precise currents to the electrochemical system of interest. All data was collected and interpreted with the help of the Gamry Framework software.

Throughout the laboratory component of the experiment, nitrile gloves, lab coats, and splash goggles were used for personal safety. Additionally, to lessen the likelihood of electrocution by the potentiostat, the researchers held one hand behind their back when interacting with active electrodes.

In the actual experiment, the first electrode tested was the platinum electrode. Before it was inserted into the main setup (Figure 1), it was polished with alumina and milliQ water to remove any corrosion and then sonicated to remove any excess alumina. The experimental setup was then assembled as pictured in Figure 1. All electrodes were submerged in the 0.1 M H_2SO_4 solution and separated from any mutual contact. Sparging was performed with a N_2 needle to remove any excess gas. The open circuit potential and uncompensated resistance were then measured and recorded.

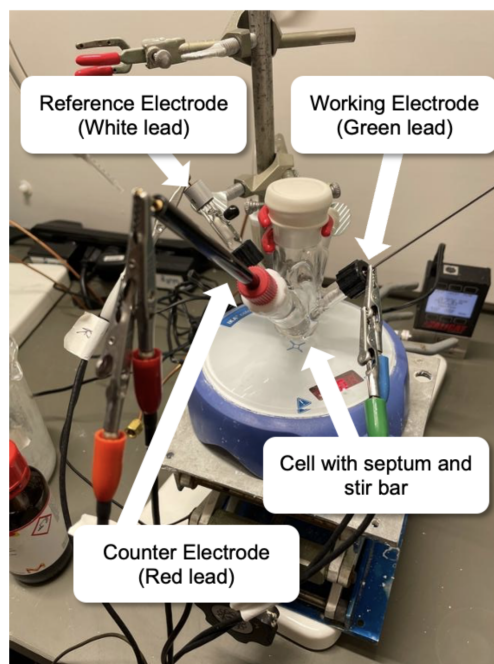


Figure 1. Experimental setup of the electrochemical cell. The three electrodes (working, reference, and counter) can be seen as well as the container in which the reaction took place. Not immediately pictured is the nitrogen needle used for pre-reaction sparging.

Ten cycles of a cyclic voltammogram were then taken from 0 V to -0.8 V and back again, and data was recorded vs a Hg/HgSO_4 reference electrode at a scan rate of 100 mV/s . A catalytic wave was observed, and eleven points surrounding its foot were selected for

chronoamperometry. These points were evenly spaced in 25 mV intervals. Then, using the computer, the potentiostat was instructed to run the different voltages sequentially from least to greatest. Each voltage was run for 100 s and the diameter of the circular platinum surface was noted to be 2 mm for the purpose of subsequent current density calculations. Throughout the initial (platinum) experiment, continuous stirring should have been applied but was not. However, this did not significantly affect the data, per the TA and lab instructor.

The process was repeated for the Sn and Ti electrodes with stirring enabled, as it should have been. The respective areas of these rectangular electrode was measured with a hand ruler to be $6\text{ mm} \times 8\text{ mm}$ and $7\text{ mm} \times 9\text{ mm}$. The respective CVs were collected over 0 V to -1.8 V and 0 V to -1.6 V . Due to extreme corrosion and contamination of the solution with tin oxides during the tin experiment, the electrolyte solution was changed between the tin and titanium runs.

Lastly, the system was cleaned by safely disposing of the acid electrolyte solution, rinsing everything with milliQ water, and returning all components to their initial spaces.

Results and Discussion

As described above, the first step was taking cyclic voltammograms for each electrode and replotting the data on an SHE scale, and plotting the y -axis as both current and current density.

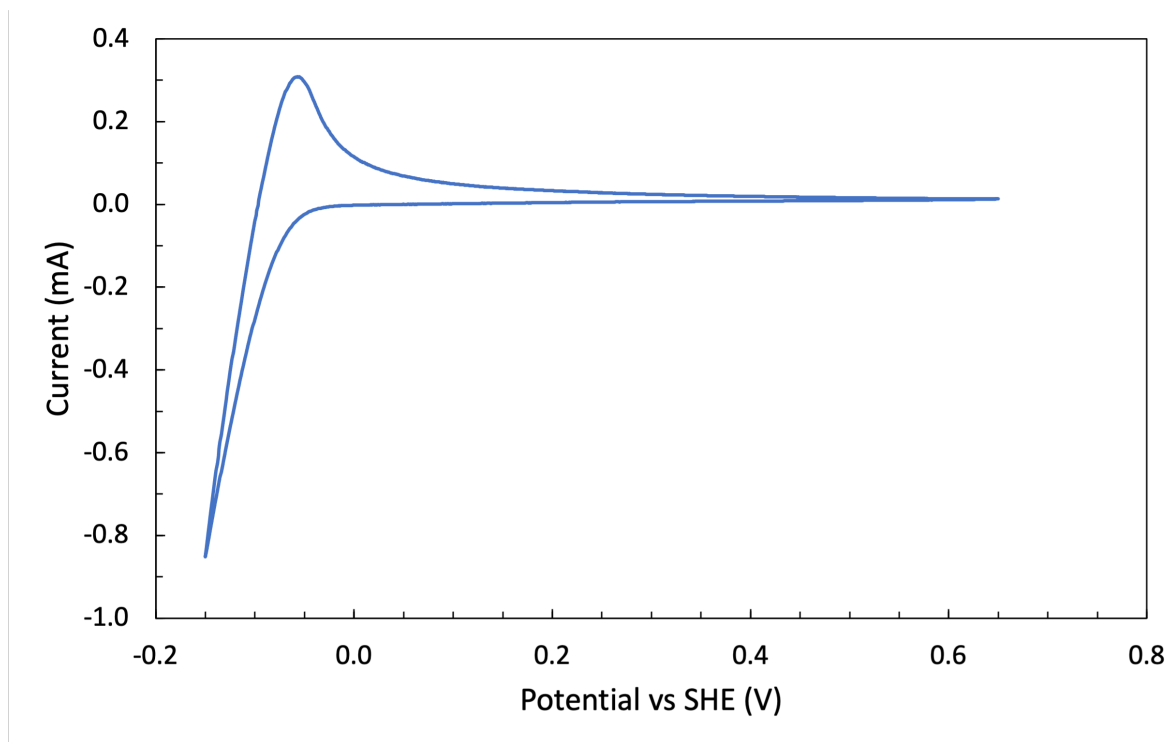


Figure 2. Extensive cyclic voltammogram exhibiting the HER over a Pt electrode in 0.1 M H_2SO_4 . The current (in mA) flowing through the working electrode was measured against the applied potential (in V) as the potential ranged from 0.65 V to -0.15 V vs SHE and back again at a scan rate of 100 mV/s. A middle curve (Curve 4) was selected as representative and plotted in Excel. The HER begins at an overpotential of 0.02 V vs SHE on the negative scan, and remaining hydrides are oxidized off of the electrode surface on the positive scan resulting in the peak between -0.1 -0 V.

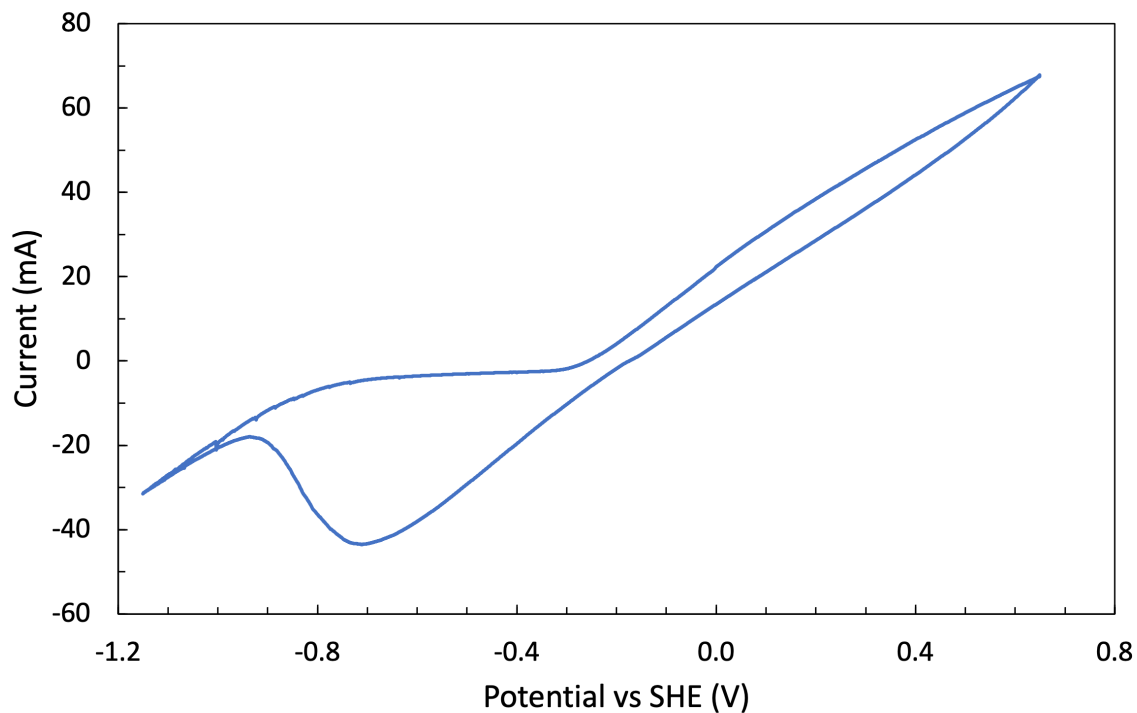


Figure 3. Extensive cyclic voltammogram exhibiting the HER over a Sn electrode in 0.1 M H_2SO_4 . The current (in mA) flowing through the working electrode was measured against the applied potential (in V) as the potential ranged from 0.65 V to -1.15 V vs SHE and back again at a scan rate of 100 mV/s. A middle curve (Curve 4) was selected as representative and plotted in Excel. The HER begins at an overpotential of 0.9 V vs SHE on the negative scan. No apparent feature correlates with the oxidation of remaining hydrides off of the electrode surface on the positive scan.

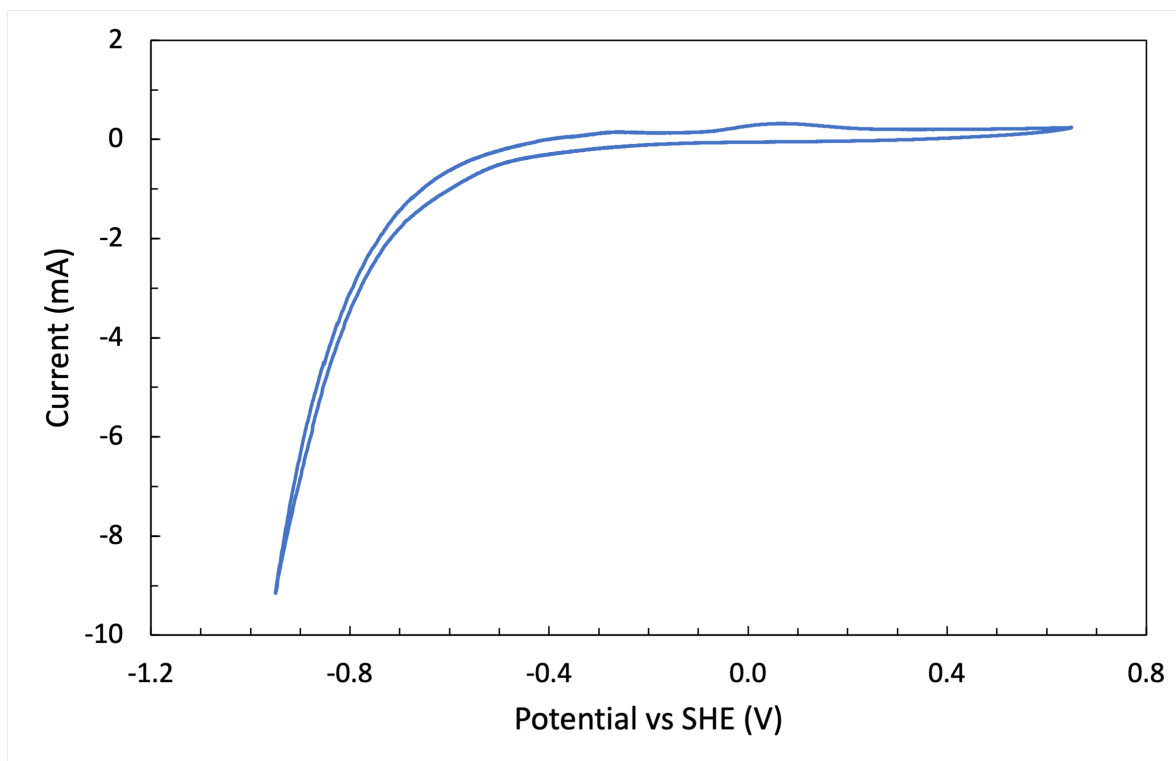


Figure 4. Extensive cyclic voltammogram exhibiting the HER over a Ti electrode in 0.1 M H_2SO_4 . The current (in mA) flowing through the working electrode was measured against the applied potential (in V) as the potential ranged from 0.65 V to -0.95 V vs SHE and back again at a scan rate of 100 mV/s. A middle curve (Curve 4) was selected as representative and plotted in Excel. The HER begins at an overpotential of 0.4 V vs SHE on the negative scan, and remaining hydrides are oxidized off of the electrode surface on the positive scan resulting in the peak between 0-0.2 V.

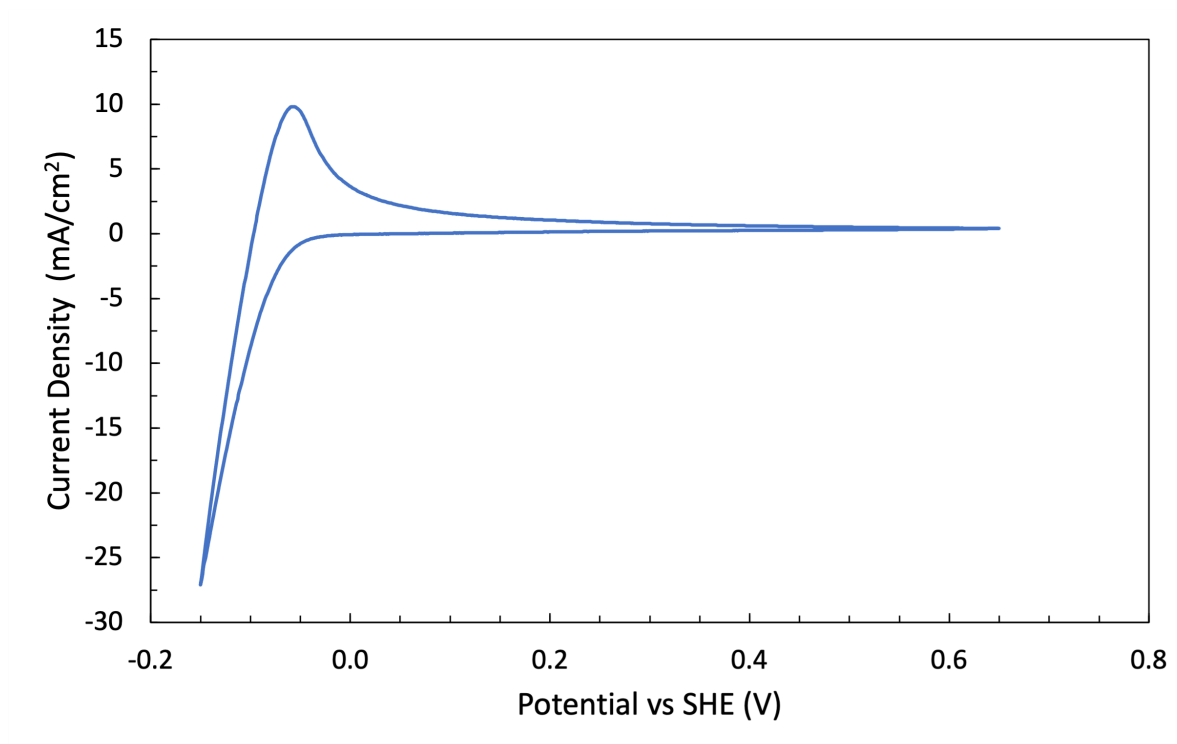


Figure 5. Intensive cyclic voltammogram exhibiting the HER over a Pt electrode in 0.1 M H_2SO_4 . The current density (in mA/cm^2) flowing through the working electrode was measured against the applied potential (in V) as the potential ranged from 0.65 V to -0.15 V vs SHE and back again at a scan rate of 100 mV/s. The surface area of the catalyst used in the normalization was 0.0314 cm^2 . A middle curve (Curve 4) was selected as representative and plotted in Excel. The HER begins at an overpotential of 0.02 V vs SHE on the negative scan, and remaining hydrides are oxidized off of the electrode surface on the positive scan resulting in the peak between -0.1 -0 V.

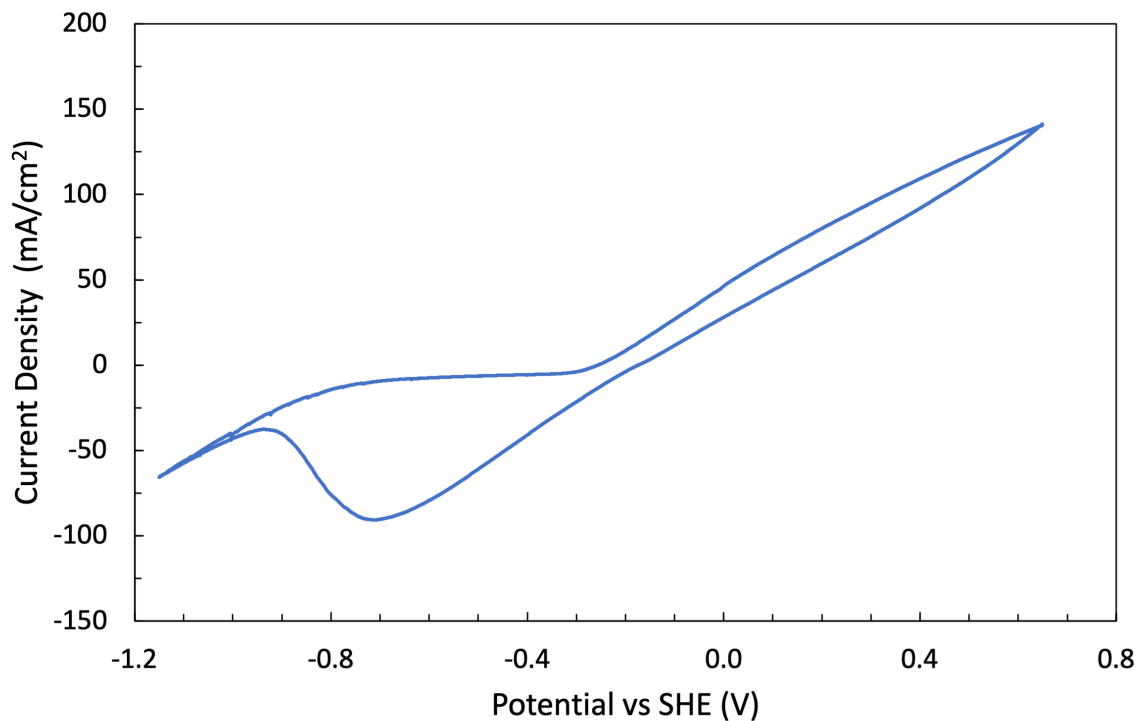


Figure 6. Intensive cyclic voltammogram exhibiting the HER over a Sn electrode in 0.1 M H₂SO₄. The current density (in mA/cm²) flowing through the working electrode was measured against the applied potential (in V) as the potential ranged from 0.65 V to -1.15 V vs SHE and back again at a scan rate of 100 mV/s. The surface area of the catalyst used in the normalization was 0.48 cm². A middle curve (Curve 4) was selected as representative and plotted in Excel. The HER begins at an overpotential of 0.9 V vs SHE on the negative scan. No apparent feature correlates with the oxidation of remaining hydrides off of the electrode surface on the positive scan.

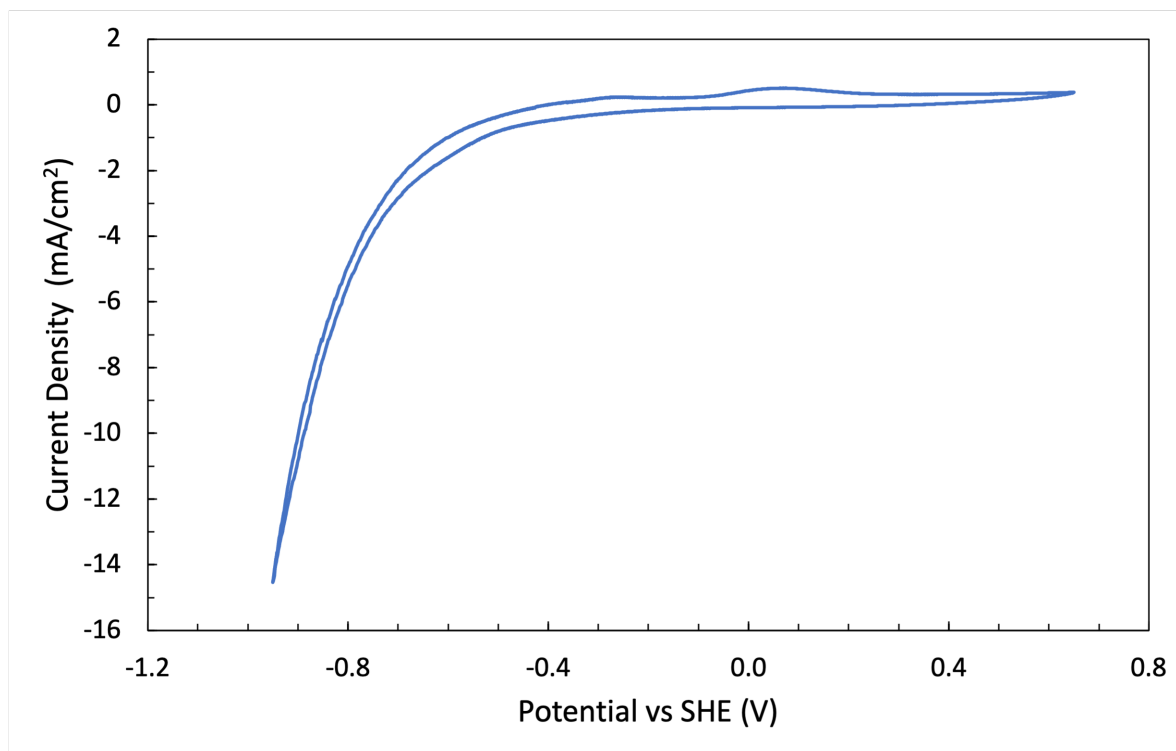


Figure 7. Intensive cyclic voltammogram exhibiting the HER over a Ti electrode in 0.1 M H_2SO_4 . The current density (in mA/cm^2) flowing through the working electrode was measured against the applied potential (in V) as the potential ranged from 0.65 V to -0.95 V vs SHE and back again at a scan rate of 100 mV/s. The surface area of the catalyst used in the normalization was 0.63 cm^2 . A middle curve (Curve 4) was selected as representative and plotted in Excel. The HER begins at an overpotential of 0.4 V vs SHE on the negative scan, and remaining hydrides are oxidized off of the electrode surface on the positive scan resulting in the peak between 0-0.2 V.

Since H_2SO_4 is a strong diprotic acid, it is safe to assume that it fully dissociates into two equivalents of protons in aqueous solution. Thus,

$$\text{pH} = -\log[\text{H}_3\text{O}^+] = -\log(0.2) \approx 0.7 \quad (9)$$

Based on the Pourbaix diagrams, all three metals at $\text{pH} = 0.7$ cross the HER line (a) at approximately $E = 0$ V. This agrees well with the foot of the catalytic wave for platinum (see Figures 2, 5), but differs significantly for the feet of the catalytic waves for tin and titanium (see Figures 3-4, 6-7). Additionally, the Pourbaix diagram reveals that at higher potentials, the tin electrode forms tin oxides (largely SnO and SnO_2).⁵ These likely account for the significant observed corrosion, as high potentials can oxidize the tin atoms at the surface, making them susceptible to nucleophilic attack by the oxygen atoms of water molecules in solution. Note that the extreme corrosion of the tin electrode and presence of additional electrochemical processes (oxide formation) means that the CV measurement and onset potential calculation for the tin electrode is likely not reliable.

Thus, the result (supported by both the raw current and current density data) that tin is the most active HER catalyst is likely untrue. Consequently, only platinum and titanium will be considered in this analysis. Both the raw current and the current density data (in particular, the position of the onset potentials) indicate that platinum is more active.

Although it didn't matter in this case, note that the plot of current *density* vs. voltage is a more accurate reflection of the intrinsic activity of each electrode material than the plot of raw current vs. voltage. This is because naturally a larger quantity of material will transfer more electrons by virtue of sheer active site size. However, this is an *extensive* property, and normalizing for the surface area allows for the comparison of *intensive* properties of the material. These are actually characteristic and thus of greater interest and validity. See the Introduction for more detail on extensive and intensive properties.

Additionally, while normalization by the geometric surface area is good, alternate methods of normalization may yield even better data. One example is the determination of the *electrochemical active* surface area.⁶ On an atomic scale, not all sites on the surface of the electrode will be equally conducive to electrochemistry, so directly measuring which ones are can give a more accurate representation of current density.

Returning to the earlier idea of onset potential, recall that the onset potential was determined by analyzing points at the foot of the catalytic waves. This region of high change in current makes it naturally suited to collecting CA data. Thus, chronoamperograms were collected at the onset potential, at five higher potentials, and at five lower potentials. The potentials were all equally spaced 25 mV apart. This allowed for the construction of the Tafel plots below. For the exact method of construction, see the relevant Excel files.

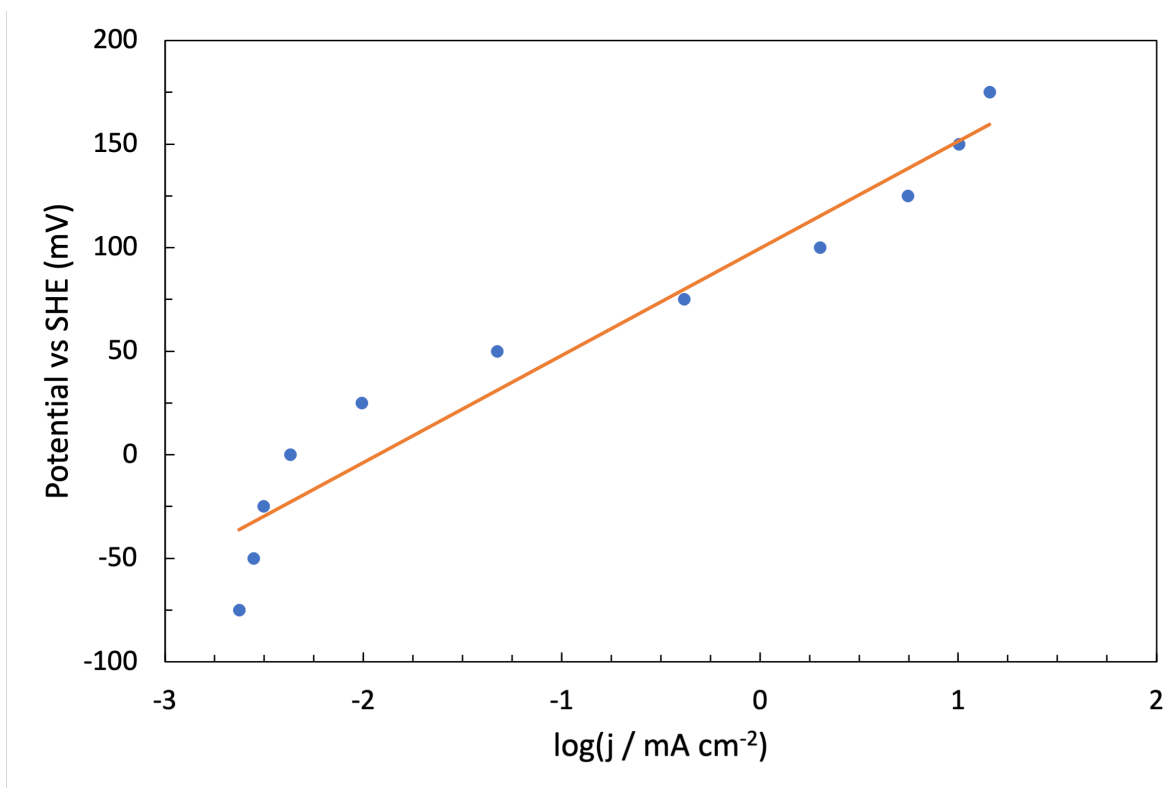


Figure 8. Tafel plot for the HER over a Pt electrode in 0.1 M H₂SO₄. The potentials (in V) were selected on the basis of preceding cyclic voltammetry experiments to surround the foot of the catalytic wave in 25 mV intervals. The logarithmic current densities were calculated from the average current measured at each potential in the last 30 s of a 100 s cyclic amperometry experiment conducted at a given potential, and normalized using the platinum electrode surface area of 0.0314 cm². Data analysis and linear regression was performed in Excel using the Solver function. A positive Tafel slope is observed: $m = 48$ mV/dec and $b = 101$ mV for a fit to $\eta = m \cdot \log(j) + b$.

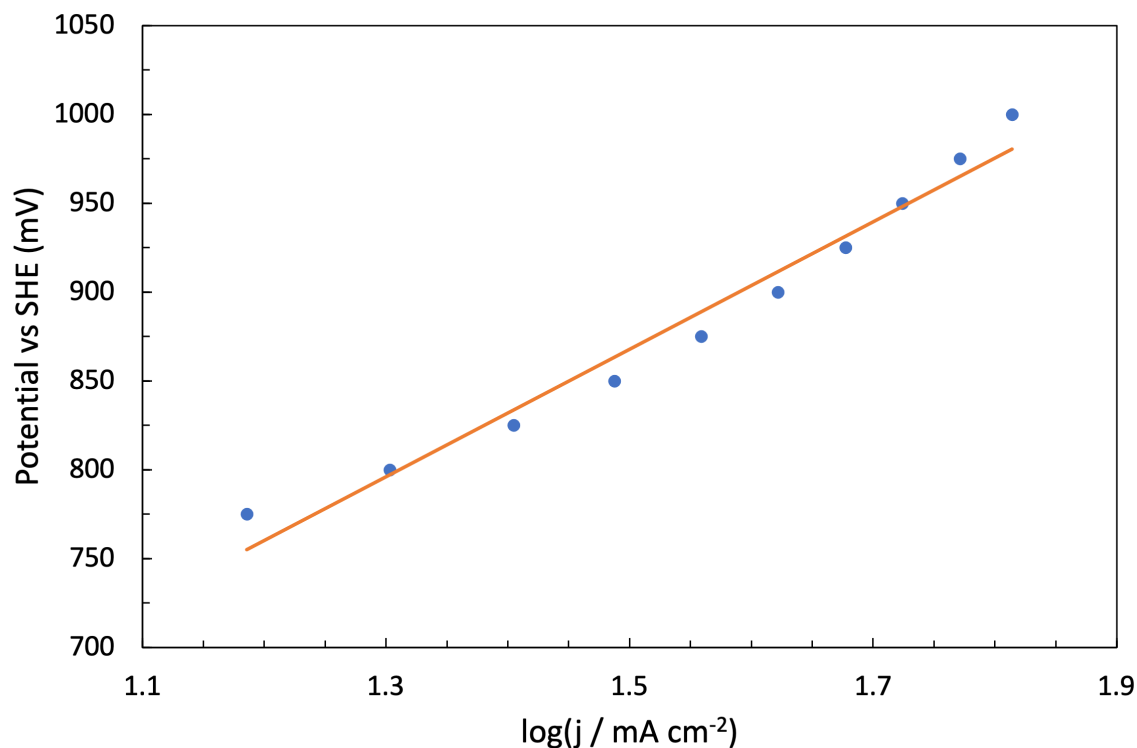


Figure 9. Tafel plot for the HER over a Sn electrode in 0.1 M H_2SO_4 . The potentials (in V) were selected on the basis of preceding cyclic voltammetry experiments to surround the foot of the catalytic wave in 25 mV intervals. The logarithmic current densities were calculated from the average current measured at each potential in the last 30 s of a 100 s cyclic amperometry experiment conducted at a given potential, and normalized using the tin electrode surface area of 0.48 cm^2 . Data analysis and linear regression was performed in Excel using the Solver function. A positive Tafel slope is observed: $m = 359 \text{ mV/dec}$ and $b = 330 \text{ mV}$ for a fit to $\eta = m \cdot \log(j) + b$.

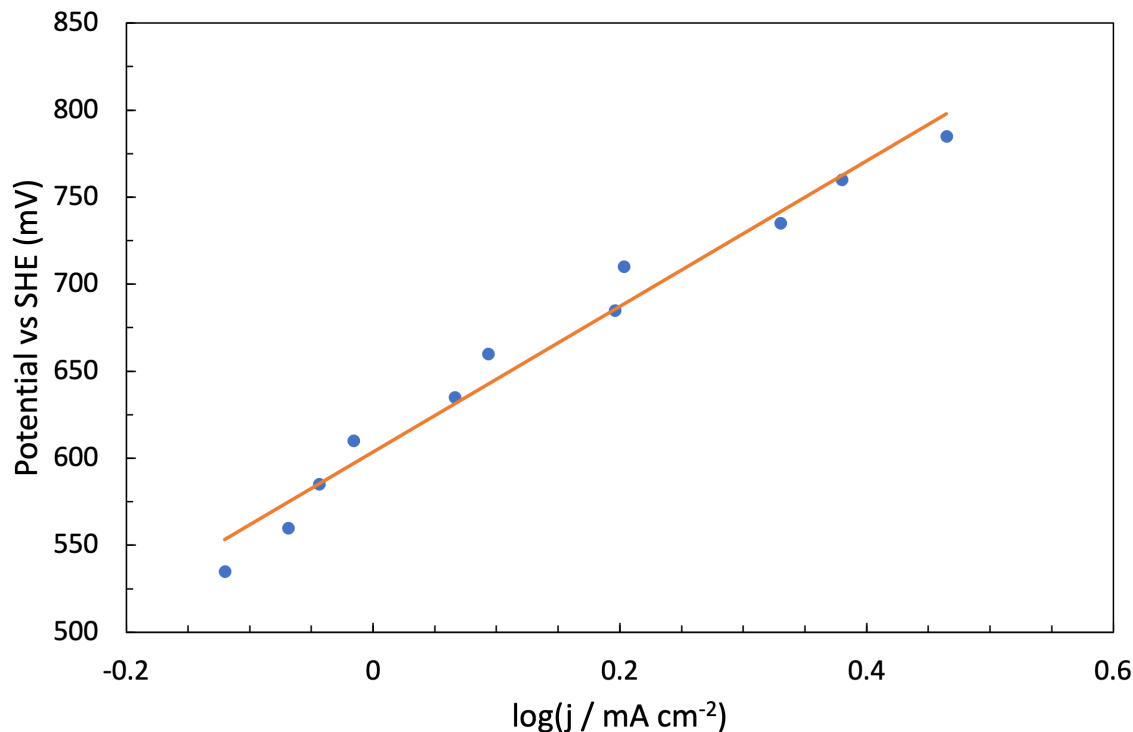


Figure 10. Tafel plot for the HER over a Ti electrode in 0.1 M H_2SO_4 . The potentials (in V) were selected on the basis of preceding cyclic voltammetry experiments to surround the foot of the catalytic wave in 25 mV intervals. The logarithmic current densities were calculated from the average current measured at each potential in the last 30 s of a 100 s cyclic amperometry experiment conducted at a given potential, and normalized using the platinum electrode surface area of 0.63 cm^2 . Data analysis and linear regression was performed in Excel using the Solver function. A positive Tafel slope is observed: $m = 402 \text{ mV/dec}$ and $b = 608 \text{ mV}$ for a fit to $\eta = m \cdot \log(j) + b$.

The Tafel slopes for platinum and tin are different. In particular, the respective slopes are $48 \text{ mV}/\log(j)$ and $359 \text{ mV}/\log(j)$. Comparing these values with the predicted Tafel slopes in the introduction reveals that platinum most likely proceeds via a V-T mechanism and thus exhibits an acid concentration dependence of 2, while tin most likely proceeds via a V-H mechanism and thus exhibits an acid concentration dependence of 1.

On rate laws, the above concentration dependence and Wuttig² imply that

$$R_{\text{Pt}} = k_1[\text{H}_3\text{O}^+]^2 e^{-\beta\eta F/RT} \quad (10)$$

and

$$R_{\text{Sn}} = k_2[\text{H}_3\text{O}^+] e^{-\beta\eta F/RT} \quad (11)$$

Lastly, it follows from the CV data (Figures 2-7) that the optimal binding energetics of the hydride intermediate should preferably be bound neither too tightly nor too loosely. This results in a “volcano plot” of transition metals, as seen in the lab manual⁴.

Conclusion

In this experiment, the onset potential was determined for each metal by finding the foot of the catalytic wave in the CV diagrams. This illustrated that Pt was the most active electrocatalyst, followed by Ti and then Sn. The foot of the catalytic wave was also used to locate points for use in chronoamperometry with the goal of constructing a Tafel plot. Said plot enabled the determination of which reaction mechanism took place over each metal (specifically Pt and Sn). In particular, it was determined that Pt makes use of the V-T mechanism while Sn makes use of the V-H mechanism. Overall, the data suggested the strong role of metal-hydride binding energetics in determining catalytic efficiency and activity.

Throughout the experiment, several sources of error likely affected results. First off, corrosion and fragmentation of the tin electrode likely drastically affected its electrochemistry. In particular, some electrons likely went toward reducing the tin oxides created on the positive sweeps, increasing the measured current. This would have also lowered the Faradaic efficiency from 100%, affecting some later calculations. Additionally, both the platinum and titanium electrodes likely undergo mild oxidation and corrosion, too, hence the requisite cleaning after each scan. Thus, the surface area is likely not constant throughout the reaction but would shrink, slightly raising the current density in later cycles. Moreover, normalization would need to be conducted in a more sophisticated manner. Furthermore, the tin and titanium electrodes were made in-house and not of the same professional caliber as the platinum electrode, so their more rudimentary form likely made the data collected on them generally less accurate as well. One last bit of experimental error is the aforementioned failure to stir the reaction during the platinum CA experiment likely made that data less than perfect, and extra cleaning of the cells between experiments would have made the data more accurate as well. On the analytical side, the models used generally gave interpretations of the data consistent with the theory. However, one particular place where they may be incomplete is indicated by the smoothness of the hypothetical curve connecting the data points in Figures 2-5 and 3-6. That the curve would be so smooth is highly unlikely statistically, and likely suggests the presence of a higher level chemical process containing more relevant information that the simplistic linear regression used does not capture.

Altogether, the data herein provides insight into the catalytic mechanism of hydrogen evolution over potential electrocatalysts, confirming the strong ability of one particular material (platinum) to catalyze said reaction and making it easier to design future experiments regarding this critical clean energy tool.

References

- (1) Seh, Z. W.; Kibsgaard, J.; Dickens, C. F.; Nørskov, I. C. J. K.; Jaramillo, T. F. Combining theory and experiment in electrocatalysis: Insights into materials design. *Science* **2017**, *355*, eaad4998.
- (2) Wuttig, A. Electrochemistry, Video lecture, Chicago, IL: University of Chicago, 2023.
- (3) Laursen, A. B.; Varela, A. S.; Dionigi, F.; Fanchiu, H.; Miller, C.; Trinhhammer, O. L.; Rossmeisl, J.; Dahl, S. Electrochemical Hydrogen Evolution: Sabatier's Principle and the Volcano Plot. *J. Chem. Educ.* **2012**, *89*, 1595–1599.
- (4) Wuttig, A.; Lant, H. Electrokinetics: Mechanism of Hydrogen Evolution on Catalytic Transition and Late Metal Electrodes, 2023.
- (5) Pourbaix, M., *Atlas of Electrochemical Equilibria in Aqueous Solutions*; National Association of Corrosion Engineers: 1440 South Creek Drive, Houston, Texas 77084, 1974.
- (6) Connor, P.; Schuch, J.; Kaiser, B.; Jaegermann, W. The Determination of Electrochemical Active Surface Area and Specific Capacity Revisited for the System MnO_x as an Oxygen Evolution Catalyst. *Z. Phys. Chem* **2020**, *234*, 979–994.